FIXTURELESS PROFILE INSPECTION OF NON-RIGID PARTS

V. Sabri*, S.A. Tahan, X.T. Pham, H. Radvar-Esfahlan, B. Louhichi, and A.M. Tahvilian
Department of Mechanical Engineering, École de Technologie Supérieure (ÉTS), Montreal, Canada
vahid.sabri.1@ens.etsmtl.ca

ABSTRACT

In order for manufacturing companies to thrive in an era of globalization, market pressures and technological developments, quality control is key. Without this aspect, it is not possible to ensure the functionality and quality of products. Due to errors that occur during the manufacturing process, manufactured parts have deviations from their nominal geometry. Therefore, one of the important aspects of the quality control of mechanical parts is geometric inspection. With the help of automated inspection, costs can be reduced during process. In our research project, we have focused on the profile inspection of non-rigid (flexible) parts. In fact, several mechanical parts used in the aeronautic and automotive industries can be considered non-rigid. This category of parts may have significantly different shapes in a *free-state* condition than the design (nominal) model due to gravity loads and residual stress. Generally, to solve this problem, special *inspection fixtures* are used in industry to compensate for the deformations of such parts to simulate the use state to perform geometric inspection. These dedicated fixtures are very expensive and the process is very time-consuming which reduces competitiveness. We aim to develop a non-rigid inspection technique to eliminate the need for specialized inspection fixtures by using a non-contact measuring system such as optical scanning and comparing the obtained point cloud from the distorted part with the nominal model to identify deviations. Using a non-rigid registration method and finite element analysis, we will apply a virtual (numerical) inspection fixture instead of a physical fixture. The simulated displacement will be performed with improved boundary conditions for simulating unfixed parts.

Keywords: quality control, geometric inspection, profile tolerance, registration, non-rigid part, assembly conditions

* Corresponding Author

1 INTRODUCTION

Following manufacturing, product geometric inspection has an important role to play in the quality control of mechanical parts. This usually consumes a large part of production lead time. Geometric specifications and product design are specified regarding functionality by means of Geometric Dimensioning and Tolerancing (GD&T). The GD&T inspection process is applied to verify the conformity of manufactured parts with specifications defined at the design stage. A reliable, efficient, and automated inspection process will decrease product life cycle time and improve industrial competition [1]. Although geometric inspection methods and equipment for rigid parts with regular geometric features have been highly improved and are generally available in the industry [2], the geometric inspection of non-rigid parts with free-form surfaces has not been well studied.

In mechanical engineering applications, surfaces are assigned profile tolerance to control variations [2]. A surface profile should be controlled based on the principles and methods established by the *ASME Y14.5-2009* standards [3] (section 8). According to these standards (or *ISO 1101:2004* standards [4]), all tolerances are applied in a free-state condition unless otherwise specified. Exemptions to this rule are given for non-rigid parts. Non-rigid parts may deform significantly from their defined tolerances due to their weight or the release of residual stresses resulting from the manufacturing processes (free-state condition) [3, 5].

Generally, to solve the above-mentioned problem, special inspection fixtures are used in the industry to compensate for the deformations of such parts to simulate use state to perform geometric inspection. These dedicated fixtures are very expensive, heavy, and complex. The process is extremely time-consuming which reduces competitiveness. The mentioned standards also allow for the application of reasonable force (not exceeding the force expected under normal assembly conditions) to create a deformation to conform non-rigid parts within the specified tolerances. The solution is to develop a fixtureless inspection technique which eliminates the need for specialized inspection fixtures by using a non-contact measuring system such as optical scanning, and comparing the obtained measurement data (point cloud) from the distorted non-rigid part with the nominal model to identify deviations.

To compare the measurement data with the nominal model, several rigid and non-rigid registration techniques have been developed such as the *Iterative Closest Point (ICP)* algorithm [6] and its variants for rigid registration; the *Multi-Dimensional Scaling (MDS)* method [7], and the *Coherent Point Drift (CPD)* algorithm [8] for non-rigid registration applied in medical imaging, animation, etc. But the situation is different for the registration of a non-rigid (flexible) mechanical part because of its *compliance behavior* (flexibility).

Knowledge of the compliance behavior of a non-rigid part is an important factor to consider when specifying tolerances and evaluating the geometric and dimensional specifications of the part. According to the definition proposed by Abenhaim *et al.* [9], the compliance behavior of a non-rigid part is a relative notion based on the ratio between an applied force and its induced displacement. Based on this definition, a compliance behavior scale (Figure 1) was proposed to classify parts based on their compliance behavior into three zones. Based on the displacements of parts in each zone (indicated in Table 01) induced by a reasonable force during inspection (40 N), the parts in zone A / B / C are considered rigid / non-rigid (flexible) / extremely non-rigid. Our research is done on typical non-rigid parts in zone B that need only elastic deformation to be conformed onto the inspection fixture or the assembly. This category includes most of the parts applied in the aeronautic and automotive industries.

In the following, this paper includes four sections; a review of previous researches for the fixtureless geometric inspection of non-rigid parts, the developed method, case study, and a conclusion.

Figure 1: A compliance behavior scale [9]

Table 1: Displacement of parts in each zone induced by a force during inspection, and their compliance behavior, indicated in [9]

Zone	Displacement by a reasonable force during inspection (40 N)	Compliance behavior
A	< 5 % of the tolerance	Rigid
B	> 10 % of the tolerance	Non-rigid (Flexible)
C	≫ Tolerance (the shape is dependent on the part's orientation and weight, such as seals and tissue)	Extremely Non-rigid

2 REVIEW OF PREVIOUS RESEARCH

Ascione and Polini [10] deals with the free-form surface inspection of non-rigid parts with inspection fixtures combined with CMM. Abenhaim *et al.* [9] presents a review of the previous approaches for the fixtureless inspection of non-rigid parts and proposes a classification of the specification methods used for the GD&T of non-rigid parts under the ASME and ISO standards. In the following, we will introduce the primary methods, based on the simulated displacement approach, developed for the geometric inspection of non-rigid parts without the use of inspection fixtures.

For the first time in 2006, Weckenmann *et al.* [11, 12] made strides in the fixtureless inspection of non-rigid parts by proposing the *virtual distortion compensation* method in which they virtually deformed the distorted part into the nominal (CAD) model by displacing the point cloud captured by a non-contact scanning device. A triangle mesh of the surface from the point cloud was generated and transformed into a finite element analysable (FEA) model. Then, the fixation process was simulated using information about the assembly features deviation from their actual to the nominal position. This method requires human intervention to identify the correlation between certain special points and assembly conditions in order to find the boundary conditions of the FEA problem. Therefore, boundary conditions can be improved to simulate a real model of the fixation system. In addition, transforming the point cloud into a FE model is a time-consuming process with uncertainties.

In 2007, Weckenmann *et al.* [13] improved the shortcomings in their previous work by deforming the CAD model towards the measurement data in the *virtual reverse deformation* method. They enforced the boundary conditions on the CAD model using the known position of the fixation points on the scanned part. Therefore, pre-processing of the measurement data is not needed. Through this method, they decreased inspection time and obtained more precise results. FE simulation of the displacement boundary conditions on the geometrically ideal CAD model is obviously more accurate. However, the proposed method still needed human intervention to find the corresponding relationship between the CAD model and the measurement data. Moreover, the modelling of the boundary conditions in the FE dataset needs to be improved to simulate the unfixed part.

Similar to the virtual reverse deformation method, Jaramillo *et al.* [14, 15] proposed an approach which requires significantly less computing power, using the Radial Basis Functions

(RBFs) to minimize the finite element mesh density required to correctly predict part behavior. Recently in [16], they improved their method by performing the flexible part registration using only partial views from areas that have to be inspected. They applied an interpolation technique based on RBFs to calculate the estimated positions of the missing fixation points since the partially scanned data may not contain all of them.

Gentilini and Shimada [17] proposed a method for inspecting the final shape of a flexible assembly part by virtually mounting it into the assembly. First, a laser-digitized dense mesh is smoothed and decimated to make it suitable for FEA. Material properties are then determined by a calibration process if not available. Specific displacement boundary conditions are applied for FE simulation of the assembly process. Once FEA is executed, quality inspection of the simulated post-assembly shape is done using visualization tools. In addition, the simulated post-assembly shape is compared with the actual post-assembly shape for method's accuracy validation. This method can predict the final shape of an assembled flexible part, but it has the shortcomings mentioned for the virtual distortion compensation method. The polygonal mesh data needs post-processing steps, smoothing and decimation, because it suffers from uncertainties, noise and a high quantity of polygons.

Recently, Radvar-Esfahlan and Tahan [18] introduced the *Generalized Numerical Inspection Fixture (GNIF)* method which is based on the property that the inter-point shortest path (*geodesic distance*) between any two points on the parts remains unchanged during an isometric deformation (*distance preserving* property of non-rigid parts) in spite of large deformation. Taking advantage of this property, the method looks for some correspondence between the part and the CAD model. The authors used *Multidimensional Scaling (MDS)* in order to find a correspondence between two metric spaces. Then, finite element non-rigid registration (FENR) was performed knowing some boundary conditions as prior information. The geometric deviations between deformed CAD model and measurement data can be calculated after FENR. Correspondence search is completely automatic. GNIF dealt with a very general case of non-rigid inspection. In the absence of assembly conditions, authors used the borders for FENR purpose whereas this situation may not conform to assembly conditions and real use state. Boundary conditions for the simulated displacements can be improved based on assembly conditions.

In contrast to the aforementioned methods, Abenhaim *et al.* [19] proposed the *iterative displacement inspection (IDI)* algorithm that is not based on the FEA module. This method iteratively deforms the meshed CAD model until it matches the scanned data. The IDI algorithm is based on the optimal step non-rigid ICP algorithms [20] which combine rigid and non-rigid registration methods. As well, a developed identification method distinguishes surface deviations from the part's distortion. This method essentially deforms the mesh in such a manner as to ensure a smoothness that prevents concealing surface defects and measurement noise during the matching process. Aidibe *et al.* [21] improved the identification module of the IDI algorithm, by proposing the use of a maximum-normed residual test to automatically set the identification threshold. However, the IDI method has some drawbacks. Due to a lack of a FE analysis, the method depends on identifying some flexibility parameters which are dependent on thickness. In addition, they use the same number of nodes in the two point clouds.

Aidibe and Tahan [22] presented an approach that combines the curvature properties of manufactured parts with the extreme value statistic test as an identification method for comparing two data sets and to recognize profile deviation. This approach was tested on simulated typical industrial sheet metal with satisfactory results in terms of error percentage in defect areas and in the estimated peak profile deviation. As the core of the algorithm is based on the Gaussian curvature comparison, application of the method is limited to relatively-flexible parts where small deformations are predictable.

3 PROPOSED APPROACH

In terms of registration problems, the literature tells us that the best approach seems to be to search for the correspondence between two data sets (in our case, the CAD model and the scanned data). The GNIF method based on the isometric deformation [18] has some advantages, as mentioned in the previous section, that encourage us to use it to search for corresponding points between two data sets. In this paper, the boundary conditions are defined and improved, and the developed method is implemented on an industrial case study. In the following, first, the GNIF method is briefly introduced, and then, our approach with a case study and results will be presented.

3.1 Generalized Numerical Inspection Fixture (GNIF) method [18]

Figure 2 shows a deformed flexible part. Let x_i and y_i' be sequentially the point on a CAD surface and the image of x_i on the part surface in a free state; where $x_1, \dots, x_n \in X$; $y_1', \dots, y_m' \in Y$; and m, n are the sampled points representing the two spaces X and Y which are intrinsically similar despite the large deformation. In other words, it is possible to unfold one surface onto the other one without stretching it. For example, the shortest path (geodesic distance) between x_1 and x_2 remains unchanged during isometric deformation, so $d_{\widehat{x_1x_2}} = d_{\widehat{y_1'y_2'}}$. Using this property, the correspondence between the CAD model and the scanned data can be found. Therefore, the first step is to estimate the pair-wise geodesic distance between all points on the two data sets.

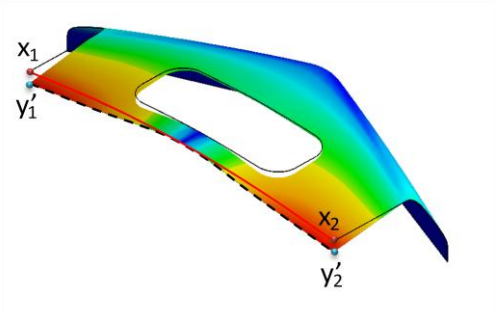

Figure 2: Intrinsic similarity in deformed shapes [18]

Let X and Y be metric spaces and $f: X \to Y$ a random map. The distortion of f is defined by:

$$dis\ f = sup_{a,b \in X} \left| d_Y\big(f(a), f(b)\big) - d_X(a,b) \right| \quad \textbf{(1)}$$

The distance $d_X(a,b)$ between a pair of points (a and b) in X is mapped to the distance $d_Y\big(f(a), f(b)\big)$ between the images of a and b under$f$. [23]

The aim is to find the correspondence between shapes X and Y with the metrics of d_X and d_Y. In most flexible part applications, the deformations are isometric. This means that two shapes X and Y, regardless of deformation, are intrinsically equal. In this case, their similarity cannot be found using rigid registration methods because the two metrics are different. One solution would be embedding two shapes in a common metric space. If this embedding can be constructed such that the Euclidean distances between all nodes remain equal in terms of geodesics, a non-rigid similarity problem is transferred into a rigid registration problem. The next issue is how to map the shapes onto a common space in an ideally isometric behavior. Mapping between two surfaces with different Gaussian curvatures (for example, a sphere and a flat surface) generates undesirable distortions. One solution to such a problem is an estimated structure that minimizes distortion as defined by Equation 1. This is the fundamental idea behind the *canonical forms* proposed in [24]. The distortion criteria in our scanned data set (point cloud) will be:

$$\sigma = max_{i,j=1,\dots,N} \left| d_{R^m}\left(f(x_i), f\big(x_j\big)\right) - d_X(x_i, x_j) \right| \quad \textbf{(2)}$$

The function σ is called *stress* in MDS literature. Historically, σ_2 has been used as the distortion criterion: Let us assume, then:

$$\sigma_2(Z; D_X) = \sum_{i>j} \left| d_{ij}(Z) - d_X(x_i, x_j) \right|^2 \quad \textbf{(3)}$$

where $Z_i = f(x_i)$ is a matrix of canonical form coordinates, $d_{ij}(Z) = d_{R^m}(z_i, z_j)$ is the Euclidean distance between the points on the canonical form, and D_X is a matrix of geodesic distances.

The minimization algorithms which minimize the stress function are known as Multidimensional scaling (MDS). Historically, MDS has been classified as a *dimensionality reduction* method. MDS always looks for a Euclidean embedding space that is seldom without distortion especially if a surface, which looks more like a sphere than a plane, is adopted to embed into a Euclidean space. To overcome this drawback, one of the surfaces (Y) is chosen as the embedding space (Figure 3). In other words, X is embedded into Y by solving the following problem:

$$min_{y_1', \ldots, y_N' \in Y} \sum \left| d_X(x_i, x_j) - d_Y(y_i', y_j') \right|^2 \quad \textbf{(4)}$$

where y_i' is the image of x_i in Y.

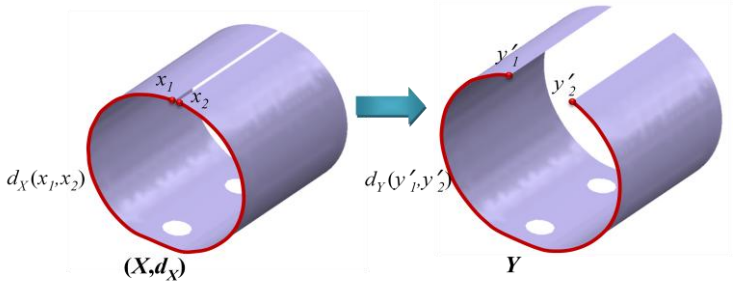

Figure 3: Generalized Multidimensional Scaling [18]

In this case, the minimum stress value determines how much the metric of X should be distorted in order to fit into Y, but contrary to MDS, there is no closed-form term for $d_Y(y_i', y_j')$ and the metric needs to be estimated, as y_i' are the optimization variables. Since $\{x_i\}$ are fixed, matrices of pair-wise geodesic distances $d_X(x_i, x_j)$ can be simply pre-calculated. But to calculate $d_Y(y_i', y_j')$, the first two points are assumed on the meshed surface $y_i = (t_i, u_i)$ and $y_i' = (t_i', u_i')$ in barycentric coordinates; any point within a triangle can be expressed as a unique convex combination of the triangle vertices. To calculate the geodesic distance between y_i and y_i', Bronstein *et al.* [25, 26] propose the three-point geodesic distance interpolation. They confirm the following equation:

$$\hat{d}_Y(y_i', y_j') = u'^T D_Y(t, t')u \quad \textbf{(5)}$$

in which, the matrix $D_Y(t, t')$ depends only on triangle indices t and t'. Substituting the interpolated distance term (Equation 5) into generalized stress function:

$$\sigma(t_1, u_1, \ldots, t_N, u_N) = \sum \left(d_X(x_i, x_j) - u_i^T D_Y(t_i, t_j) u_j \right)^2 \quad \textbf{(6)}$$

By fixing all u_j and all t_j, the stress as a function of u_i becomes *quadratic*. Consequently, by minimizing the generalized stress function, the generalized MDS problem can be solved. More details have been explained in [26] and [18].

The GNIF method uses only the borders as a corresponding relationship for matching whereas this situation generally does not conform to real use state. Boundary conditions can be improved based on assembly conditions.

3.2 Developed method based on the improvement of boundary conditions

In the present method, we calculate the Cartesian coordinates of the matching points in both the data sets (the CAD model and the scanned part); then we will improve the boundary conditions for the finite element analysis, by searching for the correspondents inside the predefined boundary areas.

The generalized MDS method of non-rigid registration, applied in the GNIF approach, represents the corresponding points in the data sets based on the barycentric coordinate system (Figure 4). But, to use these points for future purposes, their barycentric coordinates should be converted into Cartesian coordinates. Given a point with the barycentric coordinates ($\lambda_1, \lambda_2, \lambda_3$; where $\lambda_1 + \lambda_2 + \lambda_3 = 1$) inside a triangle and knowing the Cartesian coordinates of the vertices (the nodes of an element in the finite element mesh), the Cartesian coordinates can be obtained at the point through the following equations:

$$\begin{cases} x_P = \lambda_1.x_1 + \lambda_2.x_2 + \lambda_3.x_3 \\ y_P = \lambda_1.y_1 + \lambda_2.y_2 + \lambda_3.y_3 \\ z_P = \lambda_1.z_1 + \lambda_2.z_2 + \lambda_3.z_3 \end{cases} \quad \textbf{(7)}$$

By substituting $\lambda_3 = 1 - \lambda_1 - \lambda_2$ into the equations above:

$$\begin{cases} x_P = \lambda_1.x_1 + \lambda_2.x_2 + (1 - \lambda_1 - \lambda_2).x_3 \\ y_P = \lambda_1.y_1 + \lambda_2.y_2 + (1 - \lambda_1 - \lambda_2).y_3 \\ z_P = \lambda_1.z_1 + \lambda_2.z_2 + (1 - \lambda_1 - \lambda_2).z_3 \end{cases} \quad \textbf{(8)}$$

Using the Equations 8, the Cartesian coordinates of the corresponding points in each data set can be calculated.

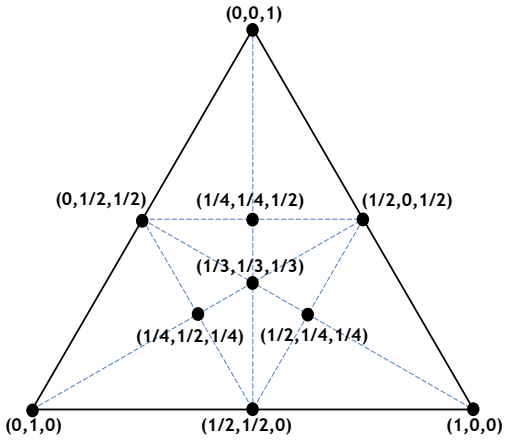

Figure 4: Barycentric coordinates $(\lambda_1, \lambda_2, \lambda_3)$ on an equilateral triangle

Figure 5 shows the different steps of our approach schematically. First, we put the scanned part surface closer enough to the CAD surface (pre-alignment) to achieve a satisfactory result for rigid registration by ICP [6]. Then, the pre-aligned surface is rigidly registered to the CAD surface by the ICP algorithm. In this step, the GNIF method is used to find the correspondents between the two surfaces.

To define a set of displacement boundary conditions for simulating the displacement from the CAD model to the rigidly registered scanned part surface, the constrained areas on the CAD model, such as fixation positions or contact surfaces, are first recognized. Then, the corresponding points (with the Cartesian coordinates) inside each area, and consequently their correspondents in the scanned data, are identified among all the correspondents obtained by the GNIF method. Next, by fitting a plane through the identified points, a centre of mass and a local normal vector are defined. To register each pair of the identified correspondents in the two data sets by simulated displacement using finite element analysis, the displacement boundary conditions should be completely defined by local translation and rotation laws [17]:

- the local normal vector ($\vec{n}$) is rotated to become parallel with the normal vector of the corresponding plane,
- the centre of mass ($\vec{x}_G$) is translated to the corresponding centre of mass on the corresponding plane.

Then, the finite element non-rigid registration (FENR) is performed between the two data sets based on the simulated displacement approach. Using ANSYS®, the CAD model is displaced towards the scanned surface applying the defined boundary conditions.

For identification of deviations, we use the *dsearchn* function in MATLAB® to calculate the shortest distance between each point in the scanned data set and the CAD data set. Therefore, we can easily find the points which are not in the tolerance.

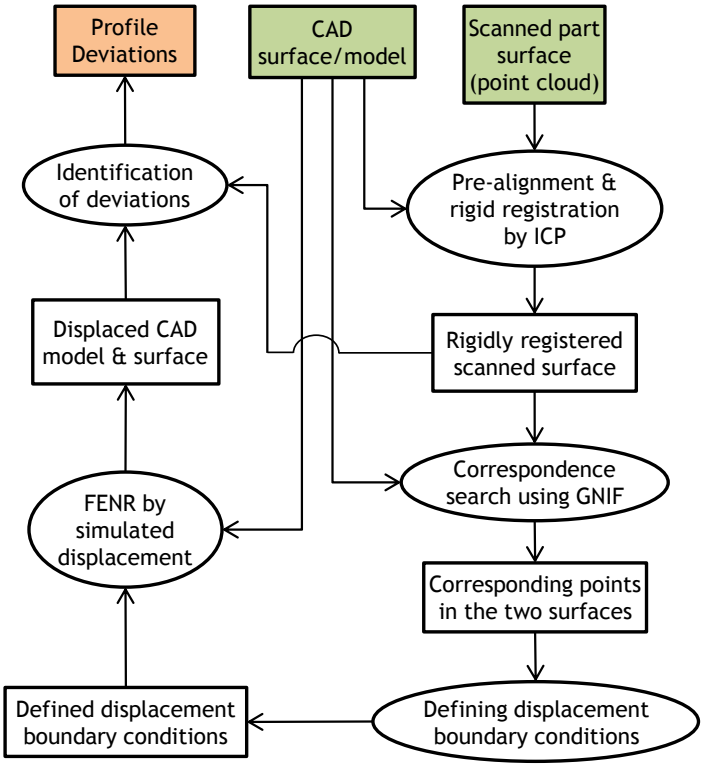

Figure 5: Flowchart of the proposed approach

4 CASE STUDY

We evaluated our approach on an industrial flexible part model from *Bombardier Aerospace Inc.* (our industrial partner) illustrated in Figure 6. A virtual part containing known deformations and deviations (bumps) is simulated, and its point cloud is extracted. First, the pre-alignment and the rigid registration by ICP are performed (Figure 7).

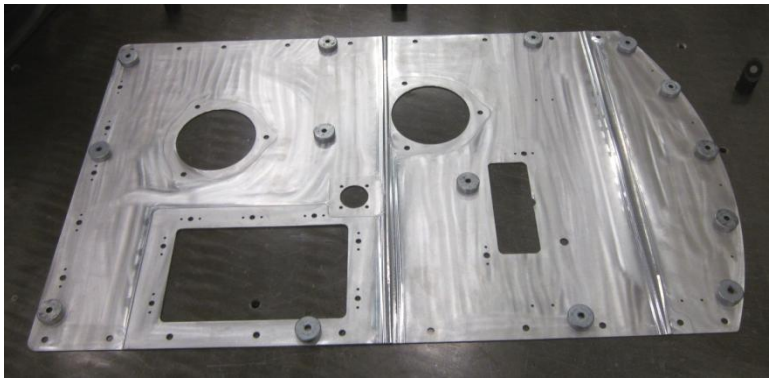

Figure 6: The flexible part, Bombardier Aerospace Inc.

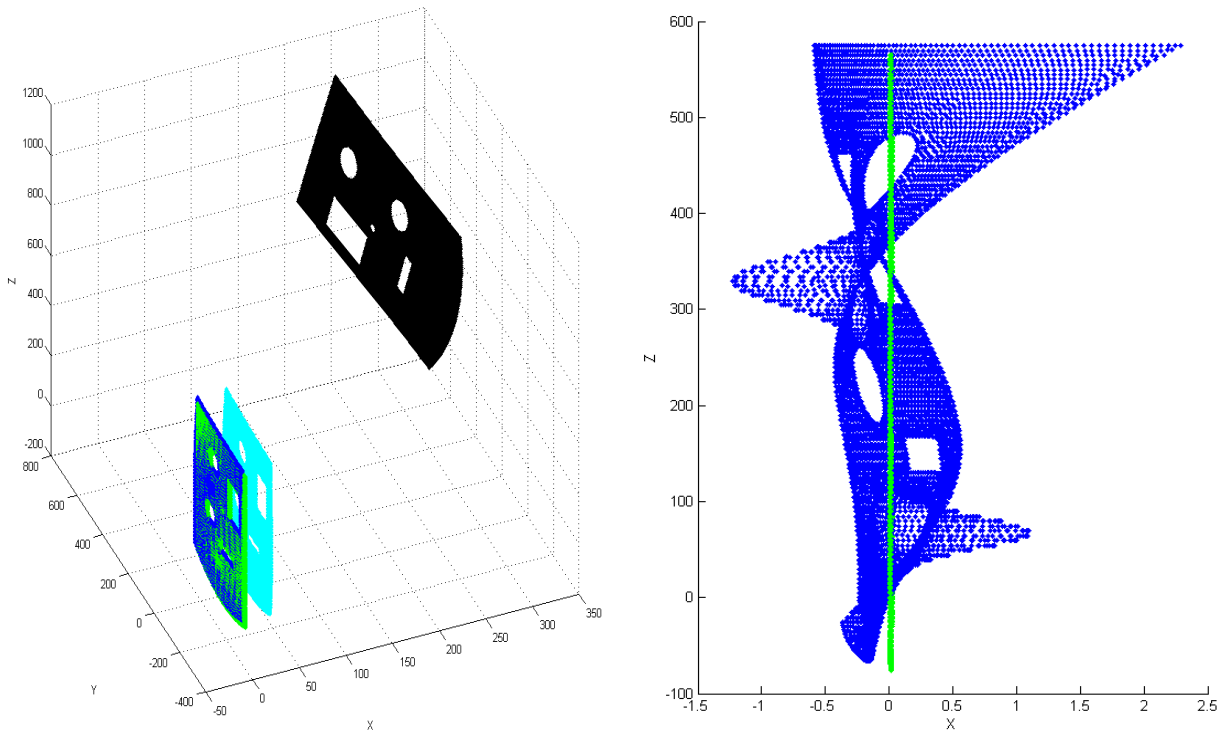

Figure 7: Pre-alignment and rigid registration by ICP; CAD surface: green, scanned part surface: black, pre-aligned surface: cyan, rigidly registered surface: blue

Using the GNIF method, the correspondents between the CAD surface and the rigidly registered surface are recognized. (Figure 8)

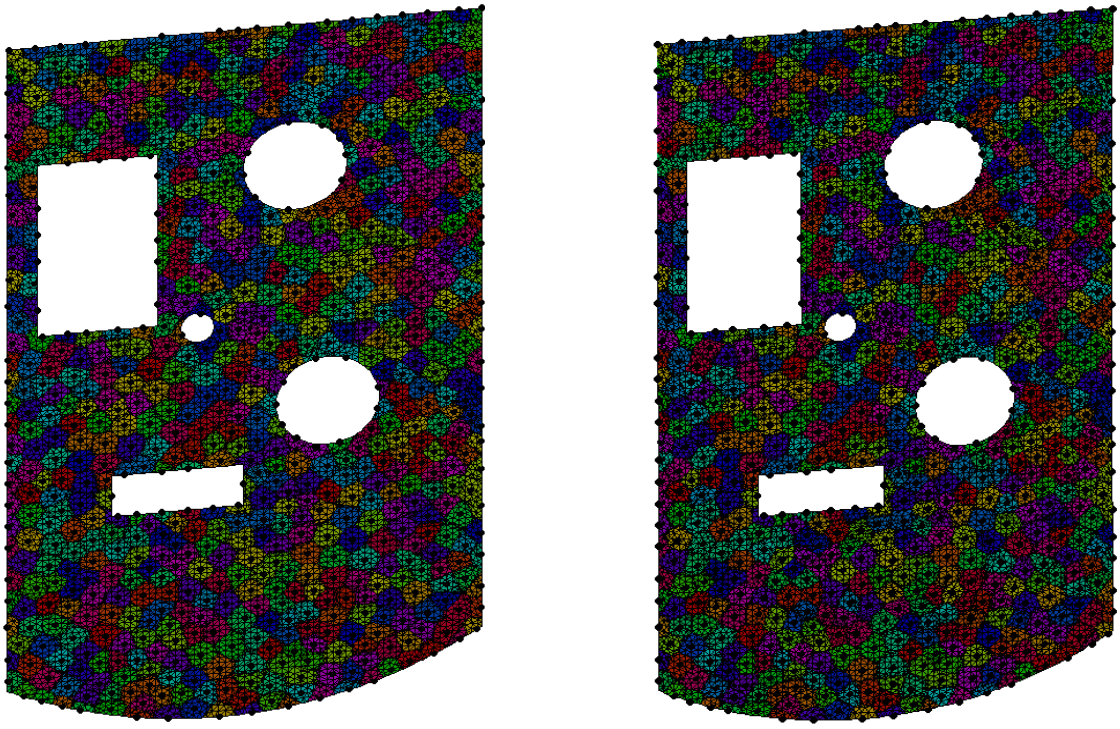

a **b**

Figure 8: Correspondence search by GNIF: a) corresponding points on the CAD surface; b) correspondents on the rigidly registered surface

Knowing the constrained areas and the corresponding points, the boundary conditions are defined. Then using ANSYS®, the CAD model is displaced to the rigidly registered scanned surface for the FE non-rigid registration applying the linear elastic FEA method. The material is *Aluminium alloy 7050-T7451*. Figure 9 shows the displacement results by FEM and the resulting deformed CAD surface.

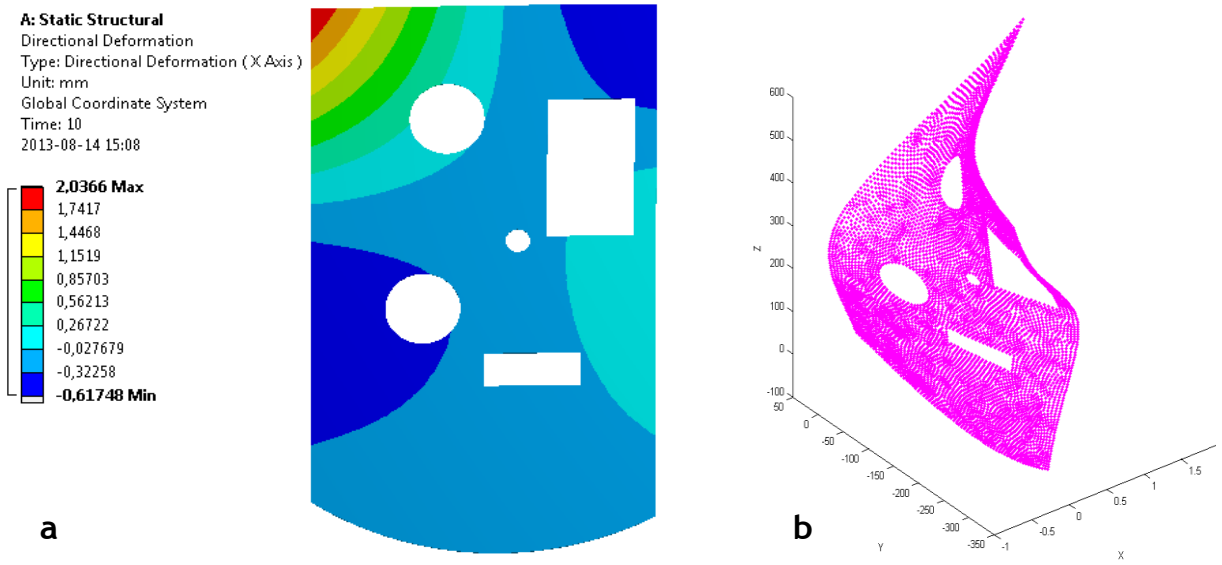

Figure 9: Finite element non-rigid registration with defined boundary conditions between the CAD model and the rigidly registered surface: a) displacement compensation by FEM in ANSYS®; b) the displaced CAD surface

Comparing the deformed CAD surface and the rigidly registered scanned surface, the known deviations are recognized. These deviations are illustrated in red in Figure 10.

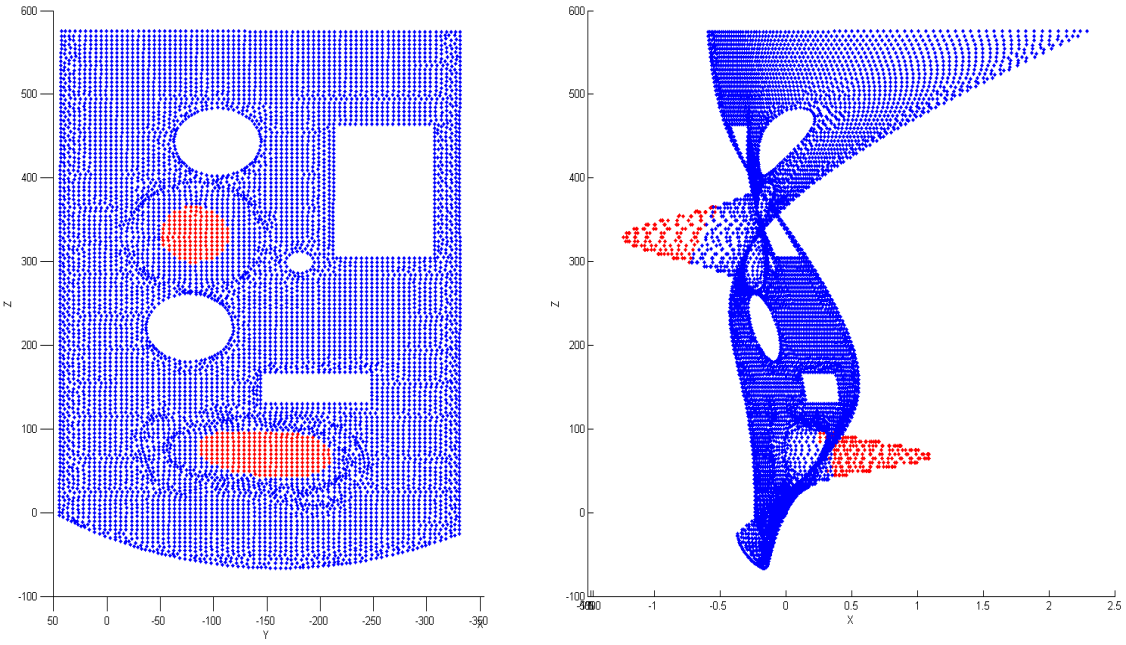

Figure 10: Identification of deviations (red points)

5 CONCLUSION

In this paper, a technique for profile inspection of flexible parts was developed to eliminate the need for specialized inspection fixtures. This approach was studied and evaluated on an industrial flexible part model from Bombardier Aerospace Inc. (our industrial partner). To

compare a point cloud (extracted from a simulated part containing known deformation and deviations) with the CAD model, first a pre-alignment and a rigid registration (using the ICP method) were performed. Next, applying the GNIF method, correspondents between the two data sets were found. Knowing the constrained areas such as contact surfaces and fixation areas on the CAD model, planes were fitted through the points inside each area as well as their correspondents on the scanned data. Then, the displacement boundary conditions were completely defined by local translation and rotation laws for finite element simulation. The position and the size of deviations were identified comparing the scanned data with the displaced CAD model. Definition of boundary conditions and consequently identification of deviations were improved in our approach. If the boundary conditions are completely and exactly defined, more precise results will be obtained. Our research progress to implement this approach on real point clouds acquired from part surfaces, to improve the definition of, and to consider different kinds of, boundary conditions. As well, we will take into account the induced force needed for conformation of flexible parts during geometric inspection.

6 ACKNOWLEDGMENTS

The authors would like to thank the National Sciences and Engineering Research Council (NSERC), Bombardier Aerospace Inc., and Creaform3D Inc. for their support and financial contribution.

7 REFERENCES

[1] **Gao, J., N. Gindy, and X. Chen, 2006.** An automated GD&T inspection system based on non-contact 3D digitization, *International journal of production research*, 44(1), pp 117-134.

[2] **Li, Y. and P. Gu, 2005.** Inspection of free-form shaped parts, *Robotics and Computer-Integrated Manufacturing*, 21(4-5), pp 421-430.

[3] ASME Y14.5-2009, 2009. *Dimensioning and tolerancing*, The American Society of Mechanical Engineers National Standard, The American Society of Mechanical Engineers, New York.

[4] ISO 1101:2004, 2004. *Geometrical product specifications (GPS)—geometrical tolerancing—tolerances of form, orientation, location and run-out*, International Organization for Standardization (ISO), Geneva.

[5] ISO 10579:2010, 2010. *Geometrical product specifications (GPS)—dimensioning and tolerancing—non-rigid parts*, International Organization for Standardization (ISO), Geneva.

[6] **Besl, P.J. and N.D. McKay, 1992.** A method for registration of 3-D shapes, *IEEE Transactions on Pattern Analysis and Machine Intelligence*, 14(2), pp 239-256.

[7] **Borg, I. and P.J.F. Groenen,** 2005. *Modern multidimensional scaling: Theory and applications*, Springer Verlag.

[8] **Myronenko, A. and S. Xubo, 2010.** Point Set Registration: Coherent Point Drift, *IEEE Transactions on Pattern Analysis and Machine Intelligence,* 32(12), pp 2262-2275.

[9] **Abenhaim, G.N., A. Desrochers, and S.A. Tahan, 2012.** Nonrigid parts' specification and inspection methods: notions, challenges, and recent advancements, *The International Journal of Advanced Manufacturing Technology*, 63(5-8), pp 741-752.

[10] **Ascione, R. and W. Polini, 2010.** Measurement of nonrigid freeform surfaces by coordinate measuring machine, *The International Journal of Advanced Manufacturing Technology*, 51(9-12), pp 1055-1067.

[11] **Weckenmann, A. and A. Gabbia,** 2006. Testing formed sheet metal parts using fringe projection and evaluation by virtual distortion compensation, *Fringe 2005*, W. Osten, Editor, Springer Berlin Heidelberg, pp 539-546.

[12] **Weckenmann, A. and J. Weickmann, 2006.** Optical inspection of formed sheet metal parts applying fringe projection systems and virtual fixation, *Metrology and Measurement Systems*, 13(4), pp 321-334.

[13] **Weckenmann, A., J. Weickmann, and N. Petrovic. 2007.** Shortening of Inspection Processes by Virtual Reverse Deformation, Proceedings of the CIRP 4th International Conference and Exhibition on Machines and Design and Production of Dies and Molds, Cesme, Izmir, Turkey, June 21-23, pp 391-398.

[14] **Jaramillo, A.E., P. Boulanger, and F. Prieto. 2009.** On-line 3-D inspection of deformable parts using FEM trained radial basis functions, Proceedings of the IEEE 12th International Conference on Computer Vision Workshops (ICCV Workshops), Kyoto, Japan, September 27-October 4, pp 1733-1739.

[15] **Jaramillo, A.E., P. Boulanger, and F. Prieto, 2011.** On-line 3-D system for the inspection of deformable parts, *The International Journal of Advanced Manufacturing Technology*, 57(9-12), pp 1053-1063.

[16] **Jaramillo, A., F. Prieto, and P. Boulanger, 2013.** Fast dimensional inspection of deformable parts from partial views, *Computers in Industry*, In Press.

[17] **Gentilini, I. and K. Shimada, 2011.** Predicting and evaluating the post-assembly shape of thin-walled components via 3D laser digitization and FEA simulation of the assembly process, *Computer-Aided Design*, 43(3), pp 316-328.

[18] **Radvar-Esfahlan, H. and S.A. Tahan, 2012.** Nonrigid geometric metrology using generalized numerical inspection fixtures, *Precision Engineering*, 36(1), pp 1-9.

[19] **Abenhaim, G.N., S.A. Tahan, A. Desrochers, and R. Maranzana, 2011.** A Novel Approach for the Inspection of Flexible Parts Without the Use of Special Fixtures, *ASME, Journal of Manufacturing Science and Engineering*, 133(1), pp 011009-011011.

[20] **Amberg, B., S. Romdhani, and T. Vetter, 2007.** Optimal Step Nonrigid ICP Algorithms for Surface Registration, Proceedings of the IEEE Conference on Computer Vision and Pattern Recognition, Minneapolis, MN, USA, June 17-22, pp 1-8.

[21] **Aidibe, A., S.A. Tahan, and G.N. Abenhaim, 2012.** Distinguishing profile deviations from a part's deformation using the maximum normed residual test. *WSEAS Transactions on Applied and Theoretical Mechanics*, 7(1), pp 18-28.

[22] **Aidibe, A. and S.A. Tahan, 2013.** Curvature estimation for metrology of non-rigid parts, Proceedings of the ASME 2013 International Manufacturing Science and Engineering Conference, Madison, Wisconsin, USA, June 10-14.

[23] **Burago, D., Y. Burago, and S. Ivanov**, 2001. *A course in metric geometry*, Vol. 33, American Mathematical Society Providence.

[24] **Elad, A. and R. Kimmel, 2003.** On bending invariant signatures for surfaces, *IEEE Transactions on Pattern Analysis and Machine Intelligence*, 25(10), pp 1285-1295.

[25] **Bronstein, A.M., M.M. Bronstein, and R. Kimmel,** 2008. *Numerical geometry of non-rigid shapes*, Springer.

[26] **Bronstein, A.M., M.M. Bronstein, and R. Kimmel, 2006.** Efficient computation of isometry-invariant distances between surfaces, *SIAM Journal on Scientific Computing*, 28(5), pp 1812-1836.